Controlling Mass Transport in Microfluidic Devices

Jason S. Kuo and Daniel T. Chiu

Department of Chemistry, University of Washington, Seattle, Washington 98195-1700; email: chiu@chem.washington.edu

Annu. Rev. Anal. Chem. 2011. 4:275–96

First published online as a Review in Advance on March 29, 2011

The *Annual Review of Analytical Chemistry* is online at anchem.annualreviews.org

This article's doi: 10.1146/annurev-anchem-061010-113926

1936-1327/11/0719-0275$20.00

Keywords

transport phenomenon, mass transfer, diffusion, convection

Abstract

Microfluidic platforms offer exquisite capabilities in controlling mass transport for biological studies. In this review, we focus on recent developments in manipulating chemical concentrations at the microscale. Some techniques prevent or accelerate mixing, whereas others shape the concentration gradients of chemical and biological molecules. We also highlight several in vitro biological studies in the areas of organ engineering, cancer, and blood coagulation that have benefited from accurate control of mass transfer.

1. INTRODUCTION

Recent advances in microfluidics-based biochemical analysis and cellular engineering have relied on increasingly sophisticated control of mass transport. The demands of high-sensitivity analyses have necessitated more stringent control over experimental parameters. Thus, mass-transport requirements have evolved to include, for instance, measures against dilution, solute concentration, elimination of convective flows, fast yet thorough mixing, and sustained delivery of chemical gradients. In this review, we provide an overview of experimental strategies related to mass transport with the goal of inspiring readers to consider these strategies in improving their own studies. This review is structured as follows: After this introductory note, we cover ways to prevent or reduce mass transport in Section 2, ways to enhance mass transport (mixing) in Section 3, and ways to shape and deliver sustained profiles of concentration gradients in Section 4. We conclude this review by describing select biological applications from recent literature in which control of mass transport is essential to the experimental outcome.

Because mass transport is a broad subject, we restrict our discussion to the mass transport of molecules by Fickian diffusion and convection; we do not discuss particle transport. Many of these topics have recently been reviewed in different contexts, so we refer the readers to appropriate reviews for additional details.

2. WAYS TO PREVENT OR MINIMIZE MASS TRANSPORT

Mass transport in certain applications is undesirable, especially in the context of rapid dilution of minute analytes (1–3). As an example, the very act of releasing the contents of a single cell by membrane lysis to probe its biochemical constituents immediately leads to severe dilution. This dilution renders the detection of the biochemical constituents challenging. To overcome dilution, convection and diffusion to and from the bulk flow can be effectively prevented by confining the analyte inside impenetrable containers such as microwells, chambers, droplets, capsules, or vesicles. **Figure 1** illustrates these ways of minimizing mass transport (4). The containers prevent mixing of the analyte with the bulk fluid. The literature on femtoliter-size containers has been reviewed in depth elsewhere (5).

2.1. Open Wells and Enclosed Chambers

A physical, impenetrable barrier is an effective method to prevent mass transfer. A common motivation for barricading against mass transfer is to prevent cross-contamination in parallel studies, such as parallel culturing of cells (6) and drug or protein polymorph screening (7). Another common motivation is to prevent the loss of minute quantities of species, such as single proteins and their substrates or products, so that their concentrations may remain at a detectable level (8).

The use of microwells or nanovials (5, 8–17) with accessible tops and enclosed chambers with interconnecting conduits (6, 7, 18) is a typical way to set up the barricade. In addition, some wall materials, such as polydimethylsiloxane (PDMS), may allow mass transport of solvents but not of the solutes; such chambers may serve as a concentrator (7, 19).

2.2. Droplets

When reagents are compartmentalized in discrete droplets surrounded by a continuous immiscible phase, the contents of one droplet are effectively isolated from the contents of another (20, 21).

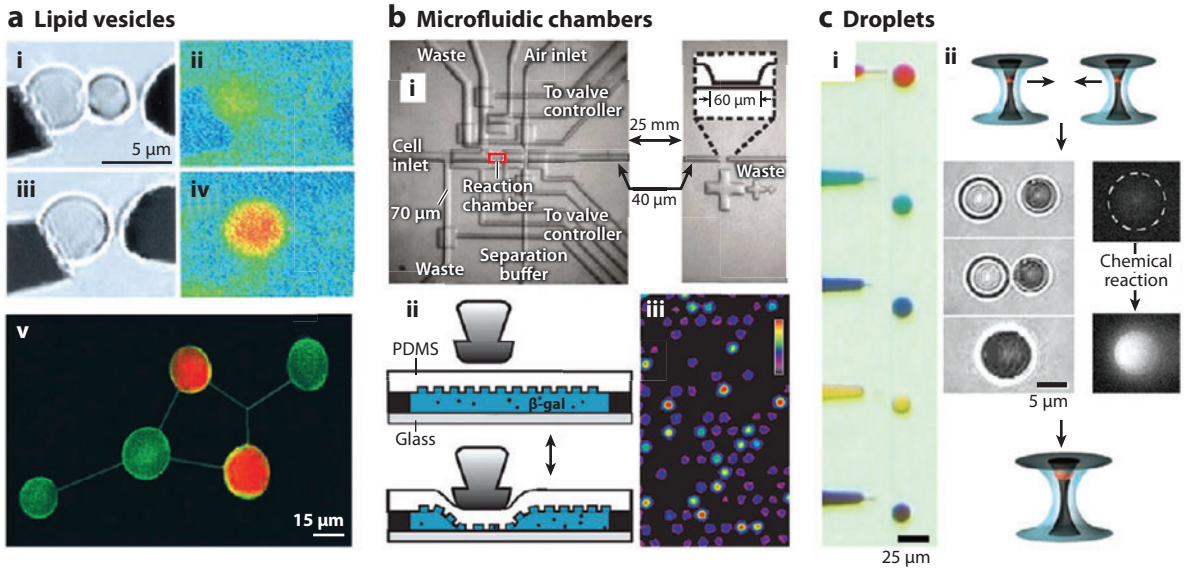

Figure 1

Ways to minimize mass transport. (*a*) Lipid vesicles. (*b*) Microfluidic chambers. (*c*) Droplets. Reprinted with permission from Reference 4. Copyright 2009, American Chemical Society.

However, this approach works only if the partition coefficient of the reagents into the continuous immiscible phase is small (2, 22).

The droplet interface is not as impervious to mass transfer as a physical, solid boundary is. Because of its high surface-to-volume ratio, a micrometer-scale droplet can have a high–mass transfer rate even with a small driving force. In some cases, the solvent in the droplet may have a small, but finite, solubility in the continuous phase. The solubility could encourage mass transport of the solvent into or out of the droplet, depending on the temperature (23). Such systems allow dynamic modulation of the droplet's volume as well as a reagent's concentration within the droplet (24). For example, cryoprotectants such as glycerol can be concentrated inside a droplet containing a cell before the cell is vitrified (25).

The extent of mixing in larger (nanoliter-scale) droplets has been quantified (26, 27). Mixing between two phases within a droplet can be achieved by, for instance, sending the droplet through a winding channel so that the interface between the phases is reoriented from the direction of movement to create an internal chaotic advection (27).

Converting a continuous stream into discrete droplets is a plausible way to overcome concentration-dispersion issues that are inherent to flow. For example, in coupling microdialysis with an analytical method such as high performance–liquid chromatography or capillary electrophoresis, Taylor dispersion can become significant when a long, large-bore tubing is used at a low flow rate (28–30). When a continuous flow is turned into a segmented flow (i.e., analyte plugs separated by oil plugs), each plug contains a discrete sampling of the original flow but is no longer subject to dispersion during transit to the analytical instrument. From this perspective, conversion of a continuous stream into droplets is analogous to digital conversion of an analog waveform; shuttling of droplets from one location to another may be viewed as a method of mass transfer that does not lead to sample loss.

2.3. Vesicles

Liposomes are synthetic lipid-bilayer vesicles that can be used to segregate nanoparticles, proteins, and DNA (31–34). A more detailed review specifically on the preparation and characterization of liposomes can be found elsewhere (35). The liposome membrane allows close mimicking of in vivo conditions while offering protection from the outside environment—liposomes are resistant even to enzymatic digestion (31). Through the use of various microfluidic platforms, monodisperse vesicles between 10 and 40 μm in diameter can be generated with a coefficient of variation as small as 5% (36). The structural integrity of the vesicles can be reinforced to the point of protecting against electroporation by filling the vesicle with poly(allyl ammonium acetate) and cross-linking it into a gel (37). The lipid vesicles can also be immobilized on surfaces to allow simplified monitoring of biochemical processes in a parallel manner (32).

Liposomes are often employed as vehicles for the delivery of drugs and can allow passive diffusion of some uncharged molecules, such as glycerol and alcohols. The diffusion can be readily monitored by surface plasmon resonance (38). The lipid-bilayer membrane is, in general, an excellent barrier against the solutes (39). However, buffer exchange (40), as well as leakage of small molecules such as calcein (36), can be accomplished by use of α-hemolysin, a bacterial toxin, to introduce ~2-nm-diameter pores. Alternatively, heating the lipid-bilayer membrane almost to the melting temperature of the constituent phospholipids induces defects in the lipid packing to permit buffer exchange or small-molecular leakage (41).

2.4. Gel Barriers and Membranes

Recent interest in tissue and organ engineering led to the use of extracellular matrix (ECM) or other gel materials to support cell growth as a way to shield against the effect of convective flow and provide a diffusive transport method. The basic configuration for in vivo cell-culturing studies involves (*a*) flow channels, (*b*) gel or permeable membrane barrier material that bridges the flow channels, and (*c*) growth of cells on one side or both sides of the barrier material. We describe two examples of the use of gels in organ engineering in Section 5.

A wide array of matrix materials are available. Collagen gels, Matrigel™ (BD Biosciences), Cultrex® BME (R&D Systems), fibrin gels, agarose gels, self-assembling peptide gels, and polyethylene glycol gels are frequently used. The choice of matrix material is based largely on the cells cultured within the experimental system (42). In particular, the gradient formation in agarose gels has been visualized using fluorescein isothiocyanate–labeled dextran (43); the gel acts as an adequate physical barrier against convection while remaining permeable to proteins. Properties of the matrix preparation (e.g., concentration, use of cross-linkers, pH) can be customized to achieve the desired permeability and elastic modulus.

2.5. Open-Volume/Virtual Containers

When fluid is emitted from parallel microchannels that are close to one another, the unconstrained streams remain unmixed for up to several millimeters or even centimeters (44–47). In this case, the streams remain parallel and segregated in the absence of any physical partitions between them, which gives rise to virtual containers (44–47).

When emitted entirely into an enclosed converging flow channel, this flow configuration resembles a laminar Y- or T-mixer (Section 3.1.1). The difference between virtual containers and a laminar mixer is that in virtual containers the mixing channel length is deliberately shortened or

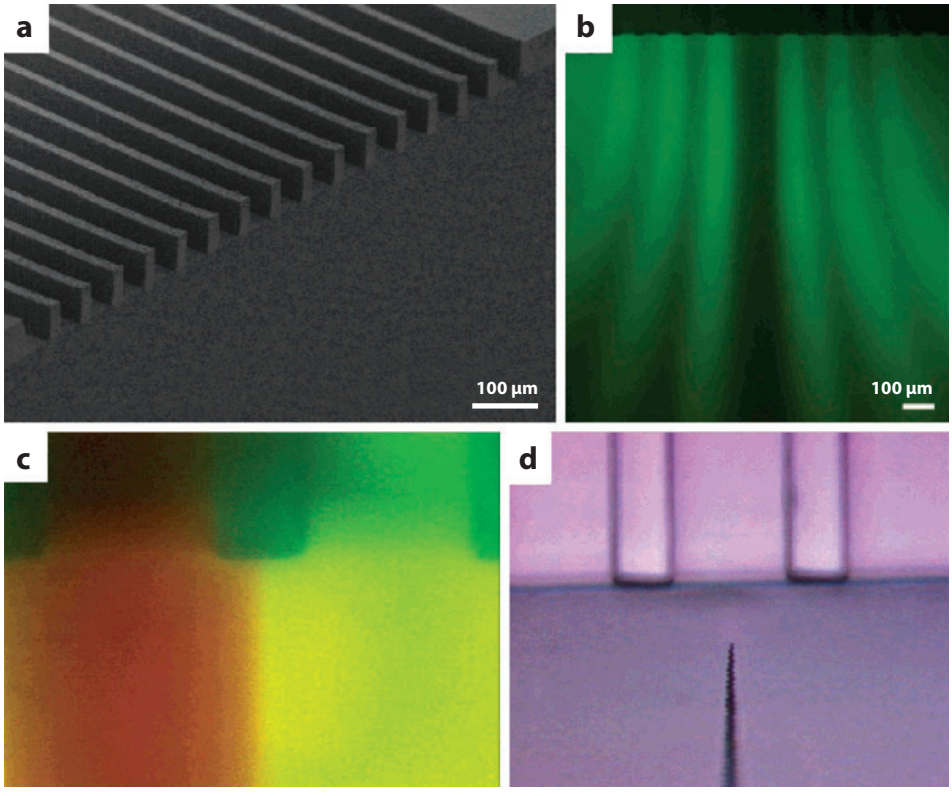

Figure 2

Open-volume approach to prevent mixing. (*a*) Scanning electron micrograph of the channel outlets leading to open volume. (*b*) Patterned flow obtained at an in-channel flow velocity of 50 mm s^{-1}. (*c*) Close-up of two channel outlets loaded with (*left*) red and (*right*) green fluorescent polystyrene microspheres flowing at 3 mm s^{-1}. (*d*) Light microscopy image of the channel outlet with a carbon-fiber nanoelectrode placed in the open volume. Reprinted with permission from Reference 44. Copyright 2004, American Chemical Society.

the device is operated at a high fluid velocity so that the convective transport in the axial direction far outweighs the lateral diffusion transport.

This approach to segregating species can also be conducted in an open volume, in which streams can remain accessible for the transfer of materials (e.g., cells or patch-clamped cells) or the insertion of probes (e.g., microelectrodes, micropipettes) (44, 48). **Figure 2** shows an open-volume microfluidic device and the profiles of the emitted streams. Patterned laminar flow in the open-volume approach has been used to generate complex concentration profiles around cells or cell fragments (44, 49–51).

3. WAYS TO ACCELERATE MASS TRANSPORT

The literature on microfluidic mixer designs has been extensively reviewed elsewhere (52–55). We briefly discuss previously reviewed designs and focus on recent developments.

The standard way to classify approaches to accelerate mass transport—that is, mixing—is to divide them into two modes of operation: passive and active (52). Passive mixers rely on geometric

features in microdevices to induce flows in directions orthogonal to the axial flow. Active mixers rely on various means to actively agitate the fluid.

3.1. Passive Mixing

In this section, we discuss various approaches and microfluidic designs used to achieve passive mixing.

3.1.1. Parallel lamination: Y- or T-mixers. Flow in microfluidic devices is largely laminar, which makes molecular diffusion the primary mode of mixing. To enhance the rate of molecular diffusion, the interfacial area between fluidic layers can be increased with chaotic advection. The fluidic motion in transverse directions can repeatedly stretch and fold the interface. Many passive mixer designs are devoted to maximizing the interfacial area by inducing various secondary flows. Depending on the fluidic phenomenon, each passive mixer design may have an optimal operating range according to Reynolds (Re) and Peclet (Pe) numbers (52). The Re number represents the ratio between the inertial momentum and the viscous forces of fluids; the Pe number represents the ratio of mass transports arising from convection and diffusion.

One of the classic mixers is to merge two incoming streams without perturbation. As the two streams concurrently flow down the microchannel, the concentration gradient between the two laminar streams induces diffusional mixing (56). The incoming streams can be positioned in a converging configuration (Y-mixer) or an opposing configuration (T-mixer) with respect to the main flow channel. The theoretical aspects of these mixers are well understood (57, 58).

Proposed improvements to this classic design include the introduction of a roughened channel wall to promote mixing (59). Narrowing of the mixing channel (e.g., entrance flow effects) (60) also causes increased mixing by compressing the stream widths; similarly, hydrodynamic focusing has also been introduced (61, 62).

Microfluidic vortices (63–65), which intrinsically have velocity components in more than one dimension, can be introduced to aid mixing in parallel lamination mixers. For example, vortices can be generated by deploying a circular (66, 67) or three-dimensional (3D) (68) mixing chamber or by adding a 90° bend to a Y-mixer (69).

3.1.2. Serial lamination (split and recombine). Split-and-recombine (SAR) mixing is a variation on the theme of lamination. In SAR mixing, the incoming streams, positioned next to one another as adjacent layers, are split in a direction perpendicular to the lamella orientation and then recombined to increase the number of lamella (70–74). In each SAR operation, the number of lamellas is successively doubled: If m is the number of SAR operations, the number of lamellas at the end is 2^m, which leads to a mixing-time improvement of (4^m-1)-fold (52). In practice, this design is more cumbersome to produce in a microfluidic format because the SAR operation ordinarily requires 3D structures (73).

The Coandă effect—the tendency of a fluid to follow a nearby surface (75)—is a way to produce SAR operations in a planar structure. Hong et al. (76) developed a planar mixer by using the Coandă effect to divide the flow, guide one of the streams at an angle, and remix the two streams to produce transverse dispersion. A sequence of four dividing-and-mixing structures (with a total length of approximately 7 mm) fully mixed the fluids at Re < 10. Design optimization with 3D Navier-Stokes analysis has been reported (75).

3.1.3. Chaotic advection: groove/herringbone. To increase the efficiency of mixing, bas-relief patterns on a channel wall, such as grooves, ridges, or herringbone, can introduce transverse

components into an otherwise unidirectional flow (77). Similar to rifling in a gun barrel, these patterns cause a spiral in the trajectory of fluid, and the resulting streamline is helical (77, 78). There are two advantages of this approach that are distinct from having a fluid flow down a helical microchannel (79). First, helical microchannels are difficult to fabricate using layer-by-layer microfabrication processes. Second, the degree of stirring in a helical channel is inefficient at Re $\ll$ 1 (Stokes's flow) (53, 77, 79).

The analytical solution of this type of mixer has been discussed in detail in the literature (80), as have optimization parameters of the design, such as the degree of asymmetry in the herringbone-shaped grooves and the amplitude of fluid rotation. Wang et al. (81) have further provided numerical simulation of this mixer. By adding embedded barriers parallel to the flow direction, Kim et al. (82) showed that the elliptic mixing pattern described by Stroock and colleagues (77, 78, 83) could be converted to a hyperbolic mixing pattern.

3.1.4. Obstacles. An alternate way to induce transverse flow is to pattern an array of obstacles in the microchannel. By strategically positioning the obstacles, it is possible to split a flow, redirect the velocity components, and recombine them. In this perspective, using obstacles in a mixer may be considered a planar implementation of a SAR mixer (mentioned above). Various geometric shapes of the obstacles have been reported. Circular (84), triangular, diamond-shaped (85), and rectangular (86) posts are capable of redirecting flows to induce mixing. The arrangement of the posts, such as in the position of the posts and separation distances, also plays a crucial role in the mixing performance. Selection of obstacle shape is important because some shapes, such as triangular, can introduce dead volumes (regions of zero velocity) at certain flow regimes (85). Obstacle mixers tend to perform better at Re $>$ 1; a key exception is the diamond shape, which yields 77% mixing at 5 mm downstream, even at Re $<$ 1 (85).

3.1.5. Beads. A simple way to introduce obstacles in a flow without having to microfabricate a dense array of obstacles in the channel is to pack the channel with microbeads (87). Microbeads split the flow, and the interstices between them serve as microvolumes for mixing. The beads, for example, can be retained by incorporating a weir into the channel. Dense packing of beads, however, can lead to a higher pressure drop than in other mixers.

3.1.6. Dean vortex. When fluid travels through a curved channel, the centrifugal effect interacts with the inertial forces to generate a radial gradient that results in a transverse flow commonly referred to as the Dean vortex (70, 88–94). **Figure 3** illustrates the evolving flow profile from a Dean vortex in a curved channel. As mentioned in Section 3.1.3, transverse flow from fluid traveling in a curved channel does not occur in the Stokes's flow regime (Re $\ll$ 1). Thus, the operation regime of a Dean vortex mixer is limited to higher Re. A more representative way to characterize the Dean vortex is to use the Dean number, $\kappa = \delta^{0.5}\mathrm{Re}$, where $\delta = d/R$, the ratio of a channel's hydraulic diameter (d) to the radius of curvature of the flow path (R). At $\kappa \sim 10$, a pair of counterrotating Dean vortices above and below the center plane of the flow channel increases mixing. At $\kappa \sim 1$, Dean vortices are not observed.

A subsequent section with the opposite curvature reverses the effect of the Dean vortex from the preceding curve. A serpentine channel, which comprises a series of opposite turns, thus results in very little mixing. To address this issue, a continuous spiral channel can be used. In this case, the Dean vortex increases as the spiral winds toward the center, where the radius of curvature is the smallest (88).

To increase the extent of mixing and improve the robustness of the designs, additional methods to induce transverse flow can be integrated into a curved channel. For example, abrupt changes

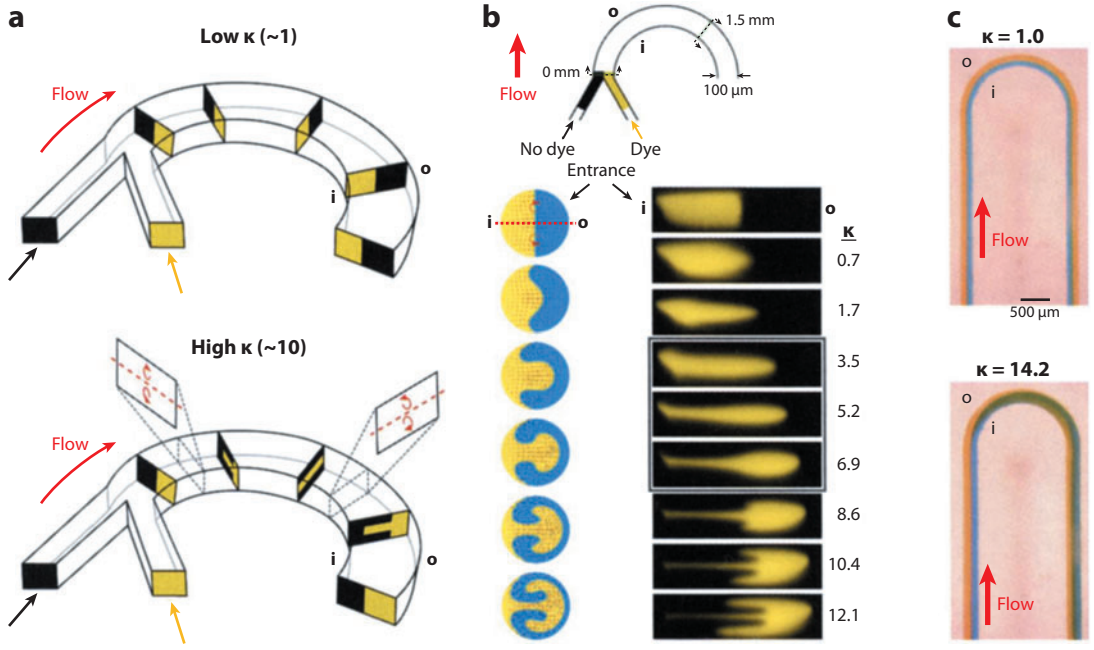

Figure 3

Dean flow phenomena in curved microchannels. (*a*) Idealized Dean flow–mediated rotation sequence. (*b*) Schematic of (*top*) the curved microchannel geometry and (*bottom*) concentration profiles. (*c*) Top-view images of two aqueous streams (*blue and orange dyes*) in a curved microchannel segment. Reprinted with permission from Reference 89. Copyright 2006, National Academy of Sciences.

in width can be incorporated into a curved flow path to induce expansion vortices (i.e., lid-driven flow) (88–90), or the flow channel can be split into multiple streams and recombined at the curves (89, 95).

3.2. Active Mixing

In this section, we discuss different methods used to achieve active mixing.

3.2.1. Cross channel: X-mixer. A simple way to disrupt the interface between two parallel layers of fluid in a main channel is to introduce a fluidic disturbance in a cross channel. The disturbance can be an oscillatory flow whose direction is orthogonal to the interface between the parallel layers. The oscillatory flow, however, has a zero-net-mass flux, so it does not cause a surge of material in the axial direction of the main channel. If the amplitude of the cross-flow is sufficient, chaotic mixing is produced, as witnessed in the stretching and folding of the interface (96). The oscillatory flow can be produced with, for example, electronic valves that control the flow of compressed air to actuate the fluidic motion. It can also be produced with electroosmotic flow (EOF) (97).

3.2.2. Time pulsing. A different way to use EOF for mixing is to alternate the injection of the incoming streams into a parallel laminate mixer. Pulsed voltages are applied such that the two incoming streams vary their individual flow rates in time but the total flow rate remains constant over time (98). For example, injection of one stream can be synchronized to a 180° phase

difference with the second stream (99) so that the injections are constantly alternating between the two streams and preventing parallel coflowing layers from developing.

The time-pulsing approach certainly is not limited to EOF. In fact, EOF imposes a serious limitation on the applicability of this approach because the reagents have to be in a compatible buffer of the appropriate strength to generate EOF in a microfluidic substrate. Artifacts arise if the reagents exhibit vastly different electrophoretic responses. To widen the applicability of the time-pulsing approach, out-of-phase peristaltic pumps can be used instead to control the fluidic injection (100).

3.2.3. Stirring. A freely rotating ferromagnetic bar can be microfabricated by photolithography and electroplating processes to stir the flow inside a microchannel (101, 102). For the sake of convenience, the microstirrer is designed to respond to a rotating external magnetic field, such as that from a laboratory stirrer–hot plate. The rotational motion is anchored around a hub; the stirrer bar is released to rotate once a copper sacrificial layer between the bar and the hub is removed by wet etching. A rotational speed of up to 600 rpm can be reliably achieved (101). A microstirrer can be used for mixing, if it is positioned in a flow channel, or for pumping, if it is positioned inside a cavity adjacent to a flow channel.

A microstirrer may be first fabricated on a silicon substrate and then sealed to a PDMS chip (101). This procedure suffers from a manual alignment step in which the microstirrer has to be positioned inside a microchannel; the resulting yield is low. A recent improvement called for using parylene as the channel-wall material because it can be put down by thin-film deposition via a bottom-up process (102). To produce a hollow channel, a thick layer of AZ 5214 photoresist temporarily fills the channel, and following the deposition of parylene, the photoresist is sacrificially removed. In this procedure, the alignment of microstructures may be performed with a mask aligner, which offers better accuracy in positioning.

The principal advantages of magnetic stirring are that (*a*) the mixing is rapid, (*b*) the technique is applicable to any fluid because the fluid and surface properties do not have to be considered, and (*c*) there is no need to tether wires. However, the microfabrication process is complex, which may limit the utility of magnetic stirrers unless they can be mass produced.

An optical stirrer approximately the size of a human red blood cell has also been reported (103). It consists of two lobes made of 3-μm silica spheres and is rotated by optical trapping. The trapping eliminates all physical connection to macroscopic hardware and allows quick reconfiguration of the design or the location of the stirrer.

3.2.4. Artificial cilia. Artificial cilia are polymer-based microactuators that respond to an electric field. A typical configuration consists of a thin polymer film (e.g., polyimide) with a thin conductive backing (e.g., chromium) positioned above an indium tin oxide electrode with a dielectric top coat (104, 105). **Figure 4** shows real and artificial cilia. When a voltage is applied, the electrostatic attraction between the electrode and the chromium layer causes the polymer film to stretch and uncurl. The rollout time depends on the applied voltage and the viscosity of the surrounding fluid; it may be as short as 7 μs in air. A life cycle of 600,000 switching cycles has been demonstrated (104).

The flow generated by the artificial cilia is a combination of a global vortex with a secondary oscillating flow. By strategically arranging the artificial cilia in a flow channel, one can generate a transverse-flow pattern resembling that from a herringbone mixer (104). As with the herringbone mixer, the operating range of artificial cilia mixers can extend below $Re < 1$. However, artificial cilia mixers have an additional benefit: The mixing can be turned on and off as needed.

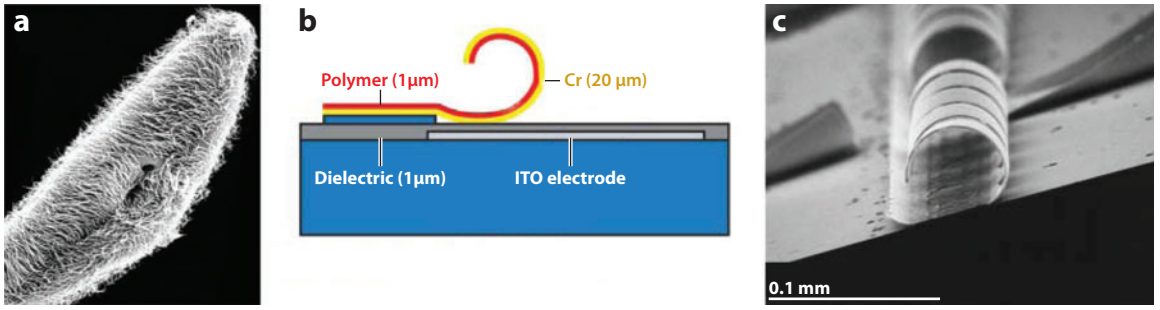

Figure 4

Real and artificial cilia. (*a*) Real cilia on a *Paramecium*. (*b*) Cross-sectional sketch of an artificial cilium. (*c*) Electron micrograph of the artificial cilia with a length of 100 μm and a width of 20 μm. Abbreviations: Cr, chromium; ITO, indium tin oxide. From Reference 104. Reproduced with permission from the Royal Society of Chemistry.

4. CONTROLLED STEADY-STATE LATERAL GRADIENT DELIVERY

Certain biological applications, such as in vitro chemotaxis and haptotaxis studies, require a specific lateral concentration profile on the microscale for a prolonged period of time, rather than fully mixed fluid or unmixed reagents. Conventional methods, such as diffusion from a pipette tip or a gel, cannot continuously achieve the same level of resolution, which may be as low as a few-percent change over a distance of 100 μm (106). In addition, the wide dynamic range and concentration function requirements (e.g., linear, power, or exponential) may impose additional technical challenges. For example, to study the dose dependency of drug effects on a cell-culture assay, a constant delivery of linear (107–112) and logarithmic concentration gradients spanning three to six orders of magnitude (113–122) is desired. **Figure 5** shows a serial diluter that can produce a gradient spanning three orders of magnitude in concentration.

Jeon et al. (106, 123) used successive blending and splitting of laminar streams in a pyramidal network of channels to demonstrate the generation of a variety of concentration profiles, for example, symmetric, asymmetric, smooth, step, and multiple peaks. This basic design has been augmented by (*a*) combining multiple gradient generators to produce functions with multiple peaks (124), (*b*) using trifurcated channels to reduce the number of mixing levels (125), and (*c*) changing the ratio of the flow rates to dynamically alter the concentration profiles (126). Other nonlinear gradients, such as power, exponential, error, Gaussian, and cubic-root functions, can be produced using a universal gradient generator. The generator allows adjustment of either the locations of the stream dividers at different levels (127) or the flow resistance in branching channels (121, 122) to achieve the desired gradient function.

Gradient delivery has been used in the chemotaxis of (*a*) neutrophils in linear gradients of interleukin-8 (123) and (*b*) endothelial cells on vascular endothelial growth factor gradients (128). Other uses of gradients include neural stem cell differentiation (129), breast cancer cell chemotaxis (130, 131), *Escherichia coli* migration (132), and rat intestinal cell migration (133). A more comprehensive review of biological applications of gradient delivery can be found elsewhere (134).

To avoid constantly exposing cells to a shear flow and washing away cell secretions in a constant laminar flow, a two-compartment diffusion chamber (ladder chamber) may be used to generate a steady-state concentration gradient across two-dimensional (2D) surfaces and 3D gels (135). The ladder chamber consists of two parallel channels that are bridged by microgrooves (2D) or gels (3D). The hydrodynamic resistance across the microgrooves or gels is significantly higher than in the main flow channels, so bulk flow remains in the main channels, and diffusion is

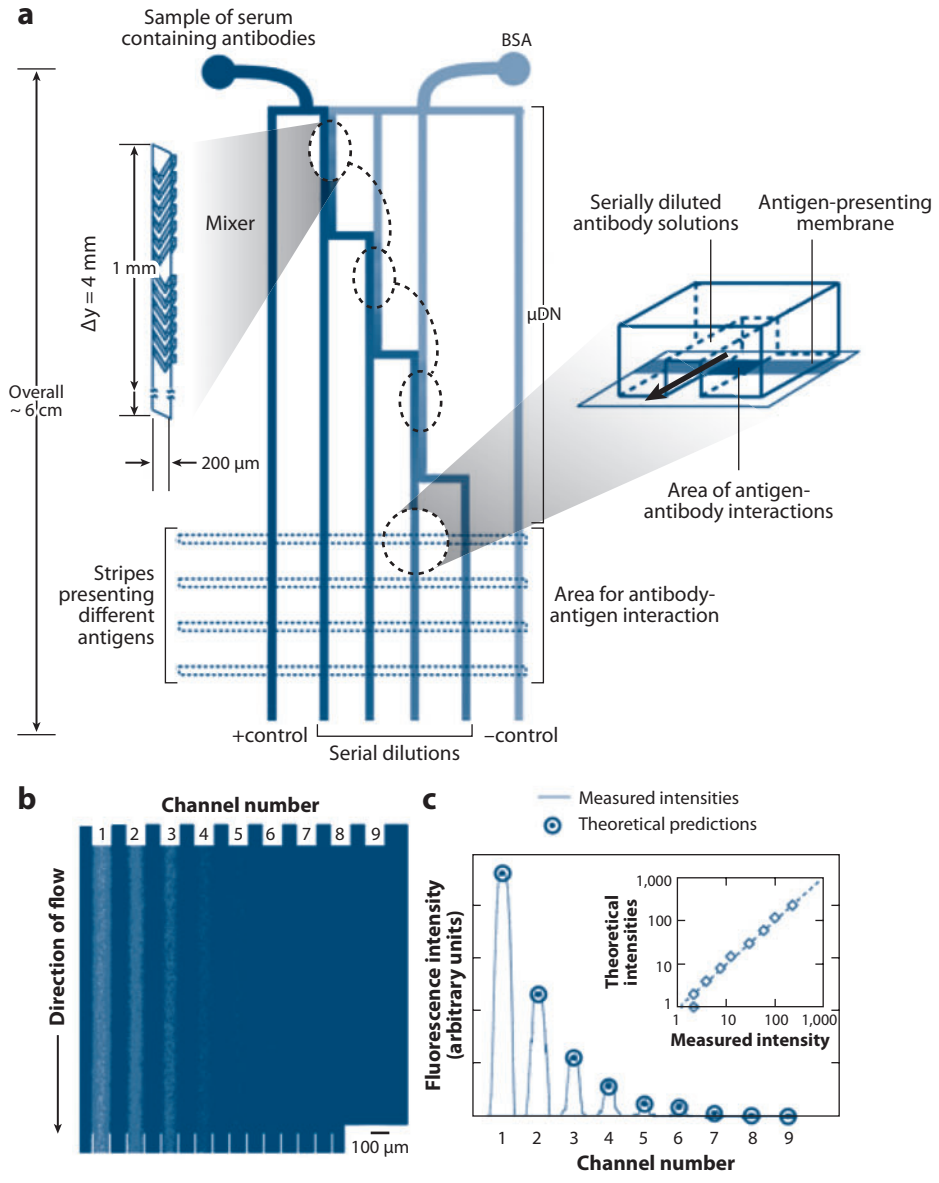

Figure 5

(*a*) Schematic representation of a gradient generator capable of serial dilution up to three orders of magnitude. (*b*) Fluorescence images of the serial dilution in a total of nine channels, where 1:1 mixing was achieved. (*c*) Measured fluorescence intensity in panel *b*. (*Inset*) The correlation between measured and calculated intensities across a dynamic range of almost 10^3. Abbreviation: BSA, bovine serum albumin. Reprinted with permission from Reference 119. Copyright 2003, American Chemical Society.

the dominant transport mechanism in the bridging microgrooves or gels. This flow resistance approach to screening out bulk flow while generating a gradient has also been used in other designs (128, 136).

Early works on gradient generation focused on the mass-conservation relationship solely between the resulting concentration profile and the number of inlet streams (124, 137). The transport process—namely a detailed hydrodynamic profile of flow in rectangular channels—was not considered; the length of each mixing channel was deliberately kept long to assure that complete diffusive mixing was achieved (106). Therefore, the sensitivity of the gradient to the operating flow rate was not fully recognized. Recently, a more comprehensive analytical model of gradient generator was presented (138, 139); this model incorporated the effects of velocity profiles and diffusion rates in the channels.

5. SELECT APPLICATIONS

In this section, we survey some of the recent innovations in microfluidic devices in which precise mass-transport control proved to be crucial to success. These examples are selected from the areas of microfluidic organ engineering, tumor cell invasion, and blood-coagulation studies.

5.1 Tissue/Organ Engineering

Below, we describe three examples in the area of tissue engineering.

5.1.1. Microfluidic lung. A bioinspired microfluidic lung can serve as an in vitro model to study the toxicity from external stimuli. Ingber and coworkers (140) recently reported a microfluidic lung that mimicked the response of the organ to bacteria and inflammatory cytokines. The microfluidic lung comprised two closely spaced channels separated by a porous flexible membrane coated with ECM. Human alveolar epithelial cells were grown on one side of the membrane, and human pulmonary microvascular endothelial cells were grown on the other side (**Figure 6**). The microfluidic lung made it possible to investigate the response of the cells while they were under cyclic mechanical strain (i.e., simulated breathing) to external stimuli such as cytokines (e.g., tumor necrosis factor α), bacterial infection, and nanoparticle inhalation.

The simulated breathing process caused an unexpected result in the transport of nanoparticles into the lung vasculature. The authors (140) observed an increase of more than a factor of four in the transport of nanoparticles across the porous membrane under breathing conditions. The cyclic stretching of the cells on the membrane had probably resulted in an altered transcellular translocation or a change in paracellular support, rather than a simple disruption of cell-cell junctions or convection across the membrane.

5.1.2. Microfluidic liver. Another organ that has been studied in the microfluidic format is the liver. Kamm and coworkers (42, 141) developed a microfluidic platform to analyze angiogenesis of rat liver cells. In this platform, two fluidic channels were separated by a collagen gel scaffold; liver and vascular endothelial cells were cultured on each side of the scaffold (**Figure 7**). The diffusion of fluorescent dextran across the scaffold suggested that the secreted proteins from the liver and vascular endothelial cells could be exchanged (141). In response to the presence of the hepatocytes, the endothelial cells formed 3D capillary-like structures that extended across the bridging gels into the hepatocyte tissues. In the absence of hepatocytes, the endothelial cells formed 2D sheet-like structures (42).

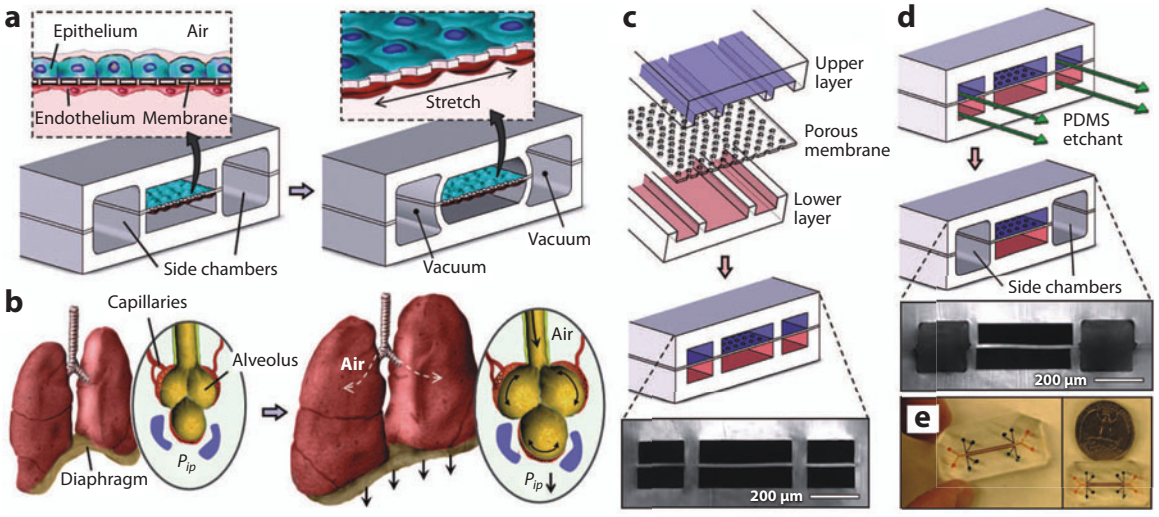

Figure 6

Biologically inspired design of a human, breathing lung-on-a-chip microdevice. (*a*) The device uses a compartmentalized polydimethylsiloxane (PDMS) microchannel to form an alveolar-capillary barrier on a thin, porous PDMS membrane coated with extracellular matrix. (*b*) Schematic of the inhalation process. (*c*) Layout of the microdevice. (*d*) After assembly, PDMS etchant is flowed through the side channels to produce two side chambers for application of a vacuum. (*e*) Images of an actual microdevice. From Reference 140. Reprinted with permission from the American Association for the Advancement of Science.

5.1.3. Tumor invasion. Tumor cell invasion into tissue and intravasation are important steps in the cancer-metastasis process. A microfluidic in vitro model allows direct observation of the invasive process and should prove to be highly useful in the future for testing drug efficacies.

Similar to the microfluidic organ experiments, tumor-invasion studies also utilize two flow channels with a bridging matrix. Chung et al. (42) seeded one channel with endothelial cells and the other with glioblastoma cells (U87MG). Within two to three days, an aggressively growing mass from the tumor cells, as well as sprouts originating from the endothelial cells, was observed.

By focusing on the chemoattractive property of epidermal growth factor (EGF), Liu et al. (142) seeded breast cancer cells (MCF-7) in the bridging matrix and subjected them to a gradient of EGF. MCF-7 cells formed long protrusions in the matrix induced by EGF; in the matrix without EGF, the cells remained round. Liu et al. (143) also witnessed the neutralizing action of matrix metalloproteinase inhibitor on tumor cells treated with EGF. In a similar microfluidic device, these authors also investigated the coculturing of salivary-gland adenoid cystic carcinoma cells and carcinoma-associated fibroblasts in a 3D matrix. Meyvantsson & Beebe (144) have extensively reviewed the current microfluidic cell-culturing models.

5.2. Blood-Coagulation Studies

Blood coagulation is a highly nonlinear phenomenon. The clotting process consists of a network of approximately 80 reactions (145) that are affected by transport processes as well as surface chemistry. Ismagilov and coworkers (146–149) used microfluidic models to elucidate the coupling

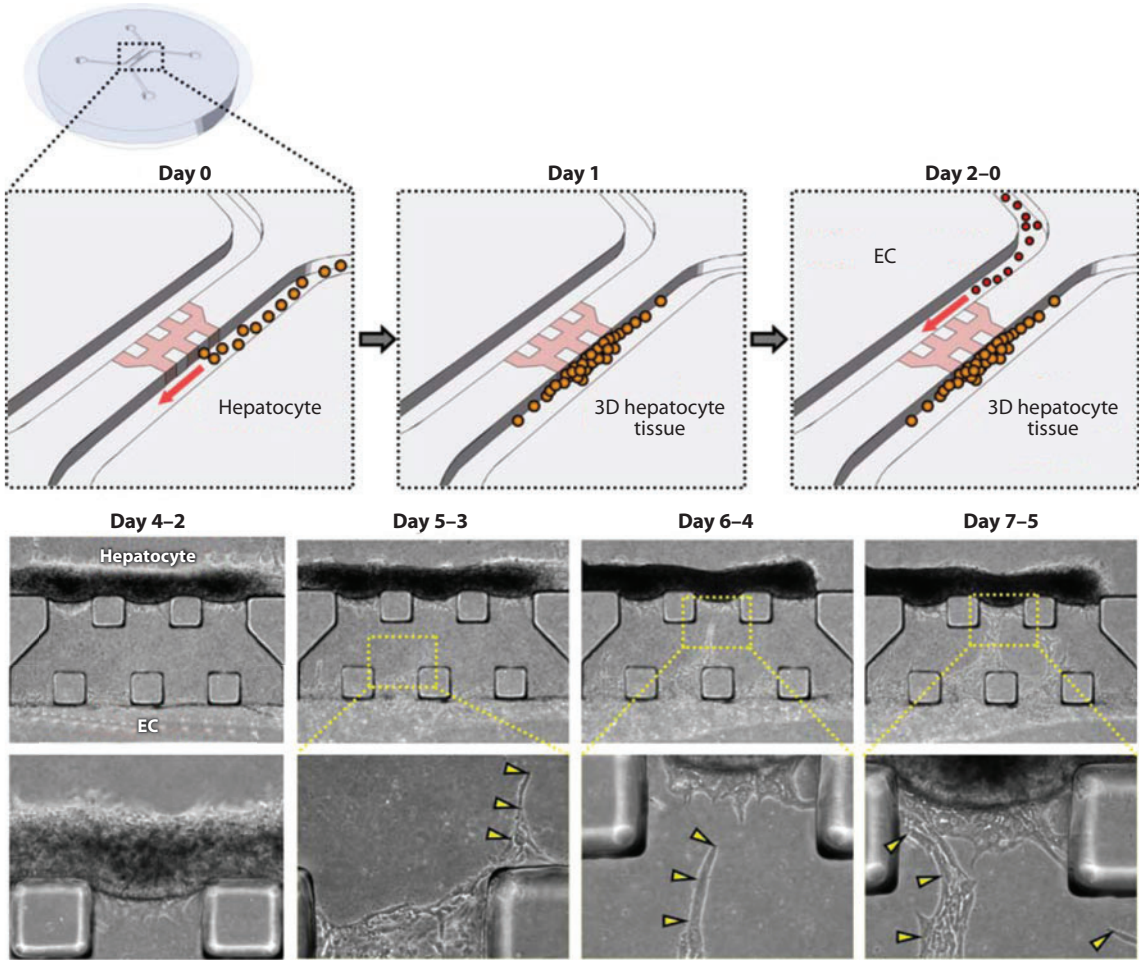

Figure 7

Hepatocyte–endothelial cell (EC) coculture in a microfluidic device. Some ECs formed vascular sprouts on day 5–3. These sprouts extended toward the three-dimensional (3D) hepatocyte tissues. Reprinted with permission from Reference 42.

of the transport process with the complex reaction pathway. The authors' experimental design involved careful control of the concentration profile of active factors under spatial confinement. A small patch of clotting stimulus (e.g., photoacid or tissue factor) was patterned on the bottom of an enclosed chamber filled with human blood plasma. The gradual accumulation of the activator (thrombin) above a certain threshold triggered the clotting (**Figure 8**).

The size of the patch dictated whether a critical concentration could be reached: When the patch was too small, diffusion of the activator away from the patch prevented a buildup of local concentration. Multiple small patches in close proximity achieved the same buildup effect as a larger patch (146). A clot propagated out of the enclosed chamber into a channel as a reaction front with a constant velocity. However, the propagation was prevented by a shear flow at the exit of the channel, which transported the buildup away by convection (148).

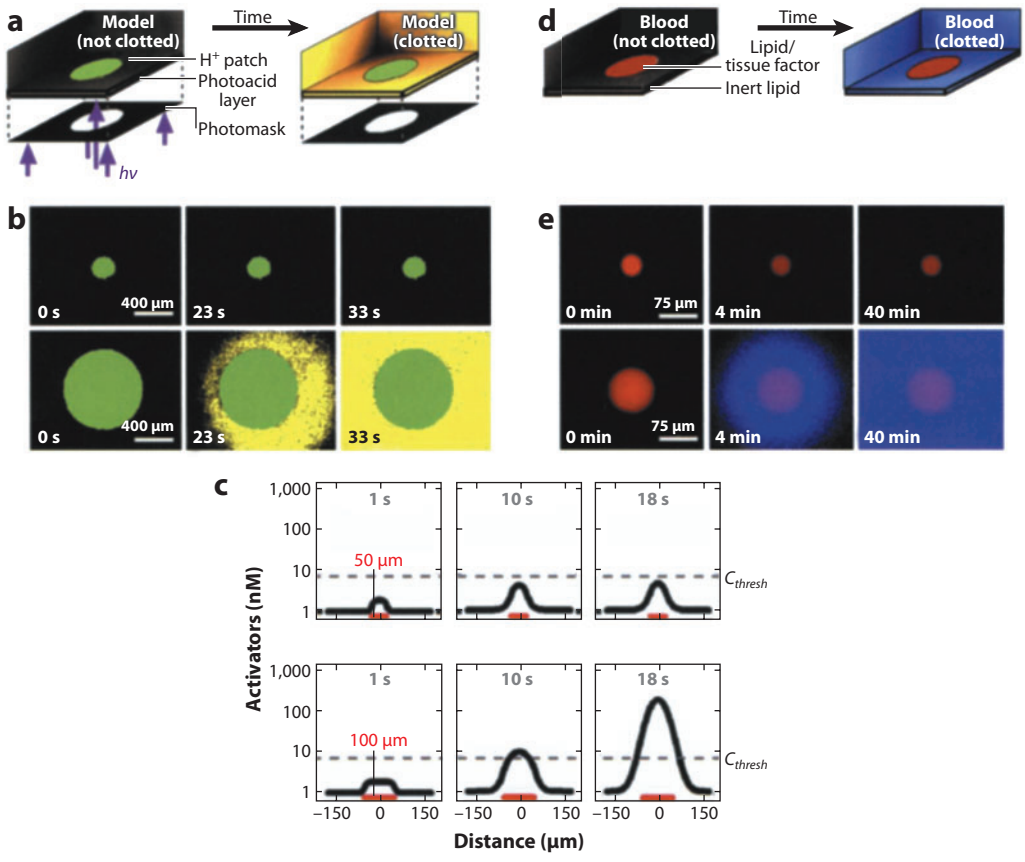

Figure 8

Experiments to study the initiation of clotting in response to patches of stimuli. (*a*) Simplified schematic of a microfluidic device. (*b*) Time-lapse fluorescence micrographs of initiation of clotting. (*c*) Numerical simulations that quantitatively describe the competition between the production of clotting activators at the patch (*red*) and diffusion of the activators away from the patch. (*d*) Schematic of an in vitro microfluidic system used to contain blood plasma and to expose it to patches of clotting stimuli. (*e*) Time-lapse fluorescence micrographs of initiation of clotting (*blue fluorescence*) on red patches. Reprinted with permission from Reference 149. Copyright 2006, National Academy of Sciences.

6. SUMMARY AND FUTURE OUTLOOK

Microfluidic devices offer precise temporal and spatial control over mass transport. New techniques to handle reagents are constantly evolving, allowing them to be segregated, mixed, or presented in a custom concentration profile sustained over time. Microfluidic structures are uniquely suited for analyzing mass transport at dimensions characteristic of biological cells. In vivo studies of chemotaxis and blood coagulation have revealed that a great deal of biological complexity can be systematically analyzed when mass transport is understood and controlled.

DISCLOSURE STATEMENT

The authors are not aware of any affiliations, memberships, funding, or financial holdings that might be perceived as affecting the objectivity of this review.

ACKNOWLEDGMENTS

We are grateful to the National Institutes of Health (NS062725, NS052637, CA147831), the National Science Foundation (CHE-0844688, CHE-0924320), and Washington State's Life Sciences Discovery Fund for their support of our work.

LITERATURE CITED

1. Chiu DT. 2003. Micro- and nano-scale chemical analysis of individual sub-cellular compartments. *Trends Anal. Chem.* 22:528–36
2. Chiu DT, Lorenz RM. 2009. Chemistry and biology in femtoliter and picoliter volume droplets. *Acc. Chem. Res.* 42:649–58
3. Allen PB, Doepker BR, Chiu DT. 2009. High-throughput capillary-electrophoresis analysis of the contents of a single mitochondria. *Anal. Chem.* 81:3784–91
4. Chiu DT, Lorenz RM, Jeffries GDM. 2009. Droplets for ultrasmall-volume analysis. *Anal. Chem.* 81:5111–18
5. Gorris HH, Walt DR. 2010. Analytical chemistry on the femtoliter scale. *Angew. Chem. Int. Ed.* 49:3880–95
6. Lee PJ, Hung PJ, Rao VM, Lee LP. 2006. Nanoliter scale microbioreactor array for quantitative cell biology. *Biotechnol. Bioeng.* 94:5–14
7. Cohen DE, Schneider T, Wang M, Chiu DT. 2010. Self-digitization of sample volumes. *Anal. Chem.* 82:5707–17
8. Rondelez Y, Tresset G, Tabata KV, Arata H, Fujita H, et al. 2005. Microfabricated arrays of femtoliter chambers allow single molecule enzymology. *Nat. Biotechnol.* 23:361–65
9. Rose D. 1999. Microdispensing technologies in drug discovery. *Drug Discov. Today* 4:411–19
10. Litborn E, Emmer A, Roeraade J. 2000. Parallel reactions in open chip-based nanovials with continuous compensation for solvent evaporation. *Electrophoresis* 21:91–99
11. Angenendt P, Nyarsik L, Szaflarski W, Glokler J, Nierhaus KH, et al. 2004. Cell-free protein expression and functional assay in nanowell chip format. *Anal. Chem.* 76:1844–49
12. Schober A, Schlingloff G, Gross A, Henkel T, Albert J, et al. 2004. Miniaturisation of synthesis and screening in nanotiterplates: the concept of NanoSynTest^{TM}. *Microsyst. Technol.* 10:281–92
13. Finnskog D, Jaras K, Ressine A, Malm J, Marko-Varga G, et al. 2006. High-speed biomarker identification utilizing porous silicon nanovial arrays and MALDI-TOF mass spectrometry. *Electrophoresis* 27:1093–103
14. Clark RA, Hietpas PB, Ewing AG. 1997. Electrochemical analysis in picoliter microvials. *Anal. Chem.* 69:259–63
15. Gorris HH, Blicharz TM, Walt DR. 2007. Optical-fiber bundles. *FEBS J.* 274:5462–70
16. Pantano P, Walt DR. 1996. Ordered nanowell arrays. *Chem. Mater.* 8:2832–35
17. Walt DR. 2010. Fibre optic microarrays. *Chem. Soc. Rev.* 39:38–50
18. Hung PJ, Lee PJ, Sabounchi P, Lin R, Lee LP. 2005. Continuous perfusion microfluidic cell culture array for high-throughput cell-based assays. *Biotechnol. Bioeng.* 89:1–8
19. Lee CC, Sui GD, Elizarov A, Shu CYJ, Shin YS, et al. 2005. Multistep synthesis of a radiolabeled imaging probe using integrated microfluidics. *Science* 310:1793–96
20. He MY, Edgar JS, Jeffries GDM, Lorenz RM, Shelby JP, Chiu DT. 2005. Selective encapsulation of single cells and subcellular organelles into picoliter- and femtoliter-volume droplets. *Anal. Chem.* 77:1539–44

21. Lorenz RM, Edgar JS, Jeffries GDM, Chiu DT. 2006. Microfluidic and optical systems for the on-demand generation and manipulation of single femtoliter-volume aqueous droplets. *Anal. Chem.* 78:6433–39
22. He MY, Sun CH, Chiu DT. 2004. Concentrating solutes and nanoparticles within individual aqueous microdroplets. *Anal. Chem.* 76:1222–27
23. Jeffries GDM, Kuo JS, Chiu DT. 2007. Controlled shrinkage and re-expansion of a single aqueous droplet inside an optical vortex trap. *J. Phys. Chem. B* 111:2806–12
24. Jeffries GDM, Kuo JS, Chiu DT. 2007. Dynamic modulation of chemical concentration in an aqueous droplet. *Angew. Chem. Int. Ed.* 46:1326–28
25. Bajpayee A, Edd JF, Chang A, Toner M. 2010. Concentration of glycerol in aqueous microdroplets by selective removal of water. *Anal. Chem.* 82:1288–91
26. Bringer MR, Gerdts CJ, Song H, Tice JD, Ismagilov RF. 2004. Microfluidic systems for chemical kinetics that rely on chaotic mixing in droplets. *Philos. Trans. R. Soc. A* 362:1087–104
27. Song H, Bringer MR, Tice JD, Gerdts CJ, Ismagilov RF. 2003. Experimental test of scaling of mixing by chaotic advection in droplets moving through microfluidic channels. *Appl. Phys. Lett.* 83:4664–66
28. Wang M, Roman GT, Perry ML, Kennedy RT. 2009. Microfluidic chip for high efficiency electrophoretic analysis of segmented flow from a microdialysis probe and in vivo chemical monitoring. *Anal. Chem.* 81:9072–78
29. Edgar JS, Milne G, Zhao YQ, Pabbati CP, Lim DSW, Chiu DT. 2009. Compartmentalization of chemically separated components into droplets. *Angew. Chem. Int. Ed.* 48:2719–22
30. Niu XZ, Zhang B, Marszalek RT, Ces O, Edel JB, et al. 2009. Droplet-based compartmentalization of chemically separated components in two-dimensional separations. *Chem. Commun.* 2009:6159–61
31. Tresset G, Takeuchi S. 2005. Utilization of cell-sized lipid containers for nanostructure and macromolecule handling in microfabricated devices. *Anal. Chem.* 77:2795–801
32. Christensen SM, Stamou D. 2007. Surface-based lipid vesicle reactor systems: fabrication and applications. *Soft Matter* 3:828–36
33. Jahn A, Vreeland WN, DeVoe DL, Locascio LE, Gaitan M. 2007. Microfluidic directed formation of liposomes of controlled size. *Langmuir* 23:6289–93
34. Chiu DT, Wilson CF, Ryttsen F, Stromberg A, Farre C, et al. 1999. Chemical transformations in individual ultrasmall biomimetic containers. *Science* 283:1892–95
35. Jesorka A, Orwar O. 2008. Liposomes: technologies and analytical applications. *Annu. Rev. Anal. Chem.* 1:801–32
36. Ota S, Yoshizawa S, Takeuchi S. 2009. Microfluidic formation of monodisperse, cell-sized, and unilamellar vesicles. *Angew. Chem. Int. Ed.* 48:6533–37
37. Robinson DB, Lee ES, Iqbal Z, Rognlien JL, Davalos RV. 2007. Reinforced vesicles withstand rigors of microfluidic electroporation. *Sens. Actuators B* 125:337–42
38. Branden M, Tabaei SR, Fischer G, Neutze R, Hook F. 2010. Refractive-index-based screening of membrane-protein-mediated transfer across biological membranes. *Biophys. J.* 99:124–33
39. Amirgoulova EV, Groll J, Heyes CD, Ameringer T, Rocker C, et al. 2004. Biofunctionalized polymer surfaces exhibiting minimal interaction towards immobilized proteins. *Chem. Phys. Chem.* 5:552–55
40. Cisse I, Okumus B, Joo C, Ha TJ. 2007. Fueling protein-DNA interactions inside porous nanocontainers. *Proc. Natl. Acad. Sci. USA* 104:12646–50
41. Monnard PA. 2003. Liposome-entrapped polymerases as models for microscale/nanoscale bioreactors. *J. Membr. Biol.* 191:87–97
42. Chung S, Sudo R, Vickerman V, Zervantonakis IK, Kamm RD. 2010. Microfluidic platforms for studies of angiogenesis, cell migration, and cell-cell interactions. *Ann. Biomed. Eng.* 38:1164–77
43. Haessler U, Kalinin Y, Swartz MA, Wu MW. 2009. An agarose-based microfluidic platform with a gradient buffer for 3D chemotaxis studies. *Biomed. Microdevices* 11:827–35
44. Olofsson J, Pihl J, Sinclair J, Sahlin E, Karlsson M, Orwar O. 2004. A microfluidics approach to the problem of creating separate solution environments accessible from macroscopic volumes. *Anal. Chem.* 76:4968–76

45. Sinclair J, Pihl J, Olofsson J, Karlsson M, Jardemark K, et al. 2002. A cell-based bar code reader for high-throughput screening of ion channel–ligand interactions. *Anal. Chem.* 74:6133–38
46. Kenis PJA, Ismagilov RF, Whitesides GM. 1999. Microfabrication inside capillaries using multiphase laminar flow patterning. *Science* 285:83–85
47. Allen PB, Milne G, Doepker BR, Chiu DT. 2010. Pressure-driven laminar flow switching for rapid exchange of solution environment around surface adhered biological particles. *Lab Chip* 10:727–33
48. Bridle H, Olofsson J, Jesorka A, Orwar O. 2007. Automated control of local solution environments in open-volume microfluidics. *Anal. Chem.* 79:9286–93
49. Granfeldt D, Sinclair J, Millingen M, Farre C, Lincoln P, Orwar O. 2006. Controlling desensitized states in ligand-receptor interaction studies with cyclic scanning patch-clamp protocols. *Anal. Chem.* 78:7947–53
50. Olofsson J, Bridle H, Sinclair J, Granfeldt D, Sahlin E, Orwar O. 2005. A chemical waveform synthesizer. *Proc. Natl. Acad. Sci. USA* 102:8097–102
51. Sinclair J, Granfeldt D, Pihl J, Millingen M, Lincoln P, et al. 2006. A biohybrid dynamic random access memory. *J. Am. Chem. Soc.* 128:5109–13
52. Nguyen NT, Wu ZG. 2005. Micromixers—a review. *J. Micromech. Microeng.* 15:R1–16
53. Stone HA, Stroock AD, Ajdari A. 2004. Engineering flows in small devices: microfluidics toward a lab-on-a-chip. *Annu. Rev. Fluid Mech.* 36:381–411
54. Ottino JM, Wiggins S. 2004. Introduction: mixing in microfluidics. *Philos. Trans. R. Soc. A* 362:923–35
55. Hessel V, Lowe H, Schonfeld F. 2005. Micromixers—a review on passive and active mixing principles. *Chem. Eng. Sci.* 60:2479–501
56. Kamholz AE, Weigl BH, Finlayson BA, Yager P. 1999. Quantitative analysis of molecular interaction in a microfluidic channel: the T-sensor. *Anal. Chem.* 71:5340–47
57. Salmon JB, Ajdari A. 2007. Transverse transport of solutes between co-flowing pressure-driven streams for microfluidic studies of diffusion/reaction processes. *J. Appl. Phys.* 101:074902
58. Wu ZG, Nguyen NT, Huang XY. 2004. Nonlinear diffusive mixing in microchannels: theory and experiments. *J. Micromech. Microeng.* 14:604–11
59. Wong SH, Bryant P, Ward M, Wharton C. 2003. Investigation of mixing in a cross-shaped micromixer with static mixing elements for reaction kinetics studies. *Sens. Actuators B* 95:414–24
60. Veenstra TT, Lammerink TSJ, Elwenspoek MC, van den Berg A. 1999. Characterization method for a new diffusion mixer applicable in micro flow injection analysis systems. *J. Micromech. Microeng.* 9:199–202
61. Knight JB, Vishwanath A, Brody JP, Austin RH. 1998. Hydrodynamic focusing on a silicon chip: mixing nanoliters in microseconds. *Phys. Rev. Lett.* 80:3863–66
62. Walker GM, Ozers MS, Beebe DJ. 2004. Cell infection within a microfluidic device using virus gradients. *Sens. Actuators B* 98:347–55
63. Lim DSW, Shelby JP, Kuo JS, Chiu DT. 2003. Dynamic formation of ring-shaped patterns of colloidal particles in microfluidic systems. *Appl. Phys. Lett.* 83:1145–47
64. Shelby JP, Lim DSW, Kuo JS, Chiu DT. 2003. High radial acceleration in microvortices. *Nature* 425:38
65. Shelby JP, Chiu DT. 2004. Controlled rotation of biological micro- and nano-particles in microvortices. *Lab Chip* 4:168–70
66. Böhm S, Greiner K, de Vries S, van den Berg A. 2001. A rapid vortex micromixer for studying high-speed chemical reactions. In *Micro Total Analysis Systems*, ed. JM Ramsey, A van den Berg, pp. 25–27. Dordrecht, Neth.: Kluwer Acad.
67. Lin CH, Tsai CH, Fu LM. 2005. A rapid three-dimensional vortex micromixer utilizing self-rotation effects under low Reynolds number conditions. *J. Micromech. Microeng.* 15:935–43
68. Long M, Sprague MA, Grimes AA, Rich BD, Khine M. 2009. A simple three-dimensional vortex micromixer. *Appl. Phys. Lett.* 94:133501
69. Yi MQ, Bau HH. 2003. The kinematics of bend-induced mixing in micro-conduits. *Int. J. Heat Fluid Flow* 24:645–56
70. Schonfeld F, Hessel V, Hofmann C. 2004. An optimised split-and-recombine micro-mixer with uniform 'chaotic' mixing. *Lab Chip* 4:65–69

71. Schwesinger N, Frank T, Wurmus H. 1996. A modulator microfluid system with an integrated micromixer. *J. Micromech. Microeng.* 6:99–102
72. Gray BL, Jaeggi D, Mourlas NJ, van Drieenhuizen BP, Williams KR, et al. 1999. Novel interconnection technologies for integrated microfluidic systems. *Sens. Actuators A* 77:57–65
73. Munson MS, Yager P. 2004. Simple quantitative optical method for monitoring the extent of mixing applied to a novel microfluidic mixer. *Anal. Chim. Acta* 507:63–71
74. Kim DS, Lee SH, Kwon TH, Ahn CH. 2005. A serpentine laminating micromixer combining splitting/recombination and advection. *Lab Chip* 5:739–47
75. Hossain S, Ansari MA, Husain A, Kim KY. 2010. Analysis and optimization of a micromixer with a modified Tesla structure. *Chem. Eng. J.* 158:305–14
76. Hong CC, Choi JW, Ahn CH. 2004. A novel in-plane passive microfluidic mixer with modified Tesla structures. *Lab Chip* 4:109–13
77. Stroock AD, Dertinger SKW, Ajdari A, Mezic I, Stone HA, Whitesides GM. 2002. Chaotic mixer for microchannels. *Science* 295:647–51
78. Stroock AD, Whitesides GM. 2003. Controlling flows in microchannels with patterned surface charge and topography. *Acc. Chem. Res.* 36:597–604
79. Liu RH, Stremler MA, Sharp KV, Olsen MG, Santiago JG, et al. 2000. Passive mixing in a three-dimensional serpentine microchannel. *J. Microelectromech. Syst.* 9:190–97
80. Stroock AD, McGraw GJ. 2004. Investigation of the staggered herringbone mixer with a simple analytical model. *Philos. Trans. R. Soc. A* 362:971–86
81. Wang HZ, Iovenitti P, Harvey E, Masood S. 2003. Numerical investigation of mixing in microchannels with patterned grooves. *J. Micromech. Microeng.* 13:801–8
82. Kim DS, Lee SW, Kwon TH, Lee SS. 2004. A barrier embedded chaotic micromixer. *J. Micromech. Microeng.* 14:798–805
83. Stroock AD, Dertinger SK, Whitesides GM, Ajdari A. 2002. Patterning flows using grooved surfaces. *Anal. Chem.* 74:5306–12
84. Wang HZ, Iovenitti P, Harvey E, Masood S. 2002. Optimizing layout of obstacles for enhanced mixing in microchannels. *Smart Mater. Struct.* 11:662–67
85. Bhagat AAS, Peterson ETK, Papautsky I. 2007. A passive planar micromixer with obstructions for mixing at low Reynolds numbers. *J. Micromech. Microeng.* 17:1017–24
86. Miranda JM, Oliveira H, Teixeira JA, Vicente AA, Correia JH, Minas G. 2010. Numerical study of micromixing combining alternate flow and obstacles. *Int. Commun. Heat Mass Transf.* 37:581–86
87. Seong GH, Crooks RM. 2002. Efficient mixing and reactions within microfluidic channels using microbead-supported catalysts. *J. Am. Chem. Soc.* 124:13360–61
88. Sudarsan AP, Ugaz VM. 2006. Fluid mixing in planar spiral microchannels. *Lab Chip* 6:74–82
89. Sudarsan AP, Ugaz VM. 2006. Multivortex micromixing. *Proc. Natl. Acad. Sci. USA* 103:7228–33
90. Lee MG, Choi S, Park JK. 2009. Rapid laminating mixer using a contraction-expansion array microchannel. *Appl. Phys. Lett.* 95:051902
91. Howell PB, Mott DR, Golden JP, Ligler FS. 2004. Design and evaluation of a Dean vortex–based micromixer. *Lab Chip* 4:663–69
92. Vanka SP, Luo G, Winkler CM. 2004. Numerical study of scalar mixing in curved channels at low Reynolds numbers. *AIChE J.* 50:2359–68
93. Yamaguchi Y, Takagi F, Watari T, Yamashita K, Nakamura H, et al. 2004. Interface configuration of the two layered laminar flow in a curved microchannel. *Chem. Eng. J.* 101:367–72
94. Jiang F, Drese KS, Hardt S, Kupper M, Schonfeld F. 2004. Helical flows and chaotic mixing in curved micro channels. *AIChE J.* 50:2297–305
95. Mouza AA, Patsa CM, Schonfeld F. 2008. Mixing performance of a chaotic micro-mixer. *Chem. Eng. Res. Des.* 86:1128–34
96. Tabeling P, Chabert M, Dodge A, Jullien C, Okkels F. 2004. Chaotic mixing in cross-channel micromixers. *Philos. Trans. R. Soc. A* 362:987–1000
97. Oddy MH, Santiago JG, Mikkelsen JC. 2001. Electrokinetic instability micromixing. *Anal. Chem.* 73:5822–32

98. Lin CH, Fu LM, Chien YS. 2004. Microfluidic T-form mixer utilizing switching electroosmotic flow. *Anal. Chem.* 76:5265–72
99. Glasgow I, Batton J, Aubry N. 2004. Electroosmotic mixing in microchannels. *Lab Chip* 4:558–62
100. Glasgow I, Aubry N. 2003. Enhancement of microfluidic mixing using time pulsing. *Lab Chip* 3:114–20
101. Lu LH, Ryu KS, Liu C. 2002. A magnetic microstirrer and array for microfluidic mixing. *J. Microelectromech. Syst.* 11:462–69
102. Ryu KS, Shaikh K, Goluch E, Fan ZF, Liu C. 2004. Micro magnetic stir-bar mixer integrated with parylene microfluidic channels. *Lab Chip* 4:608–13
103. Terray A, Oakey J, Marr DWM. 2002. Microfluidic control using colloidal devices. *Science* 296:1841–44
104. den Toonder J, Bos F, Broer D, Filippini L, Gillies M, et al. 2008. Artificial cilia for active micro-fluidic mixing. *Lab Chip* 8:533–41
105. Khatavkar VV, Anderson PD, den Toonder JMJ, Meijer HEH. 2007. Active micromixer based on artificial cilia. *Phys. Fluids* 19:083605
106. Jeon NL, Dertinger SKW, Chiu DT, Choi IS, Stroock AD, Whitesides GM. 2000. Generation of solution and surface gradients using microfluidic systems. *Langmuir* 16:8311–16
107. Hattori K, Sugiura S, Kanamori T. 2009. Generation of arbitrary monotonic concentration profiles by a serial dilution microfluidic network composed of microchannels with a high fluidic-resistance ratio. *Lab Chip* 9:1763–72
108. Cavallaro G, Maniscalco L, Campisi M, Schillaci D, Giammona G. 2007. Synthesis, characterization and in vitro cytotoxicity studies of a macromolecular conjugate of paclitaxel bearing oxytocin as targeting moiety. *Eur. J. Pharm. Biopharm.* 66:182–92
109. Babich H, Zuckerbraun HL, Weinerman SM. 2007. In vitro cytotoxicity of (-)-catechin gallate, a minor polyphenol in green tea. *Toxicol. Lett.* 171:171–80
110. Sengupta TK, Leclerc GM, Hsieh-Kinser TT, Leclerc GJ, Singh I, Barredo JC. 2007. Cytotoxic effect of 5-aminoimidazole-4-carboxamide-1-beta-4-ribofuranoside (AICAR) on childhood acute lymphoblastic leukemia (ALL) cells: implication for targeted therapy. *Mol. Cancer* 6:46
111. Hsieh FY, Tengstrand E, Lee JW, Li LY, Silverman L, et al. 2007. Drug safety evaluation through biomarker analysis—a toxicity study in the cynomolgus monkey using an antibody-cytotoxic conjugate against ovarian cancer. *Toxicol. Appl. Pharmacol.* 224:12–18
112. Tao X, Chen H, Sun XJ, Chen HF, Roa WH. 2007. Formulation and cytotoxicity of doxorubicin loaded in self-assembled bio-polyelectrolyte microshells. *Int. J. Pharm.* 336:376–81
113. Takara K, Sakaeda T, Yagami T, Kobayashi H, Ohmoto N, et al. 2002. Cytotoxic effects of 27 anticancer drugs in HeLa and MDR1-overexpressing derivative cell lines. *Biol. Pharm. Bull.* 25:771–78
114. Zhang XL, Wang W, Yu WT, Xie YB, Zhang XH, et al. 2005. Development of an in vitro multicellular tumor spheroid model using microencapsulation and its application in anticancer drug screening and testing. *Biotechnol. Prog.* 21:1289–96
115. Hassan SB, Haglund C, Aleskog A, Larsson R, Lindhagen E. 2007. Primary lymphocytes as predictors for species differences in cytotoxic drug sensitivity. *Toxicol. In Vitro* 21:1174–81
116. Yamori T, Matsunaga A, Sato S, Yamazaki K, Komi A, et al. 1999. Potent antitumor activity of MS-247, a novel DNA minor groove binder, evaluated by an in vitro and in vivo human cancer cell line panel. *Cancer Res.* 59:4042–49
117. Papagiannaros A, Hatziantonio S, Dimas K, Papaioannou GT, Demetzos C. 2006. A liposomal formulation of doxorubicin, composed of hexadecylphosphocholine (HePC): physicochemical characterization and cytotoxic activity against human cancer cell lines. *Biomed. Pharmacother.* 60:36–42
118. Gentry BG, Boucher PD, Shewach DS. 2006. Hydroxyurea induces bystander cytotoxicity in cocultures of herpes simplex virus thymidine kinase-expressing and nonexpressing HeLa cells incubated with ganciclovir. *Cancer Res.* 66:3845–51
119. Jiang XY, Ng JMK, Stroock AD, Dertinger SKW, Whitesides GM. 2003. A miniaturized, parallel, serially diluted immunoassay for analyzing multiple antigens. *J. Am. Chem. Soc.* 125:5294–95
120. Pihl J, Sinclair J, Sahlin E, Karlsson M, Petterson F, et al. 2005. Microfluidic gradient–generating device for pharmacological profiling. *Anal. Chem.* 77:3897–903
121. Lee K, Kim C, Ahn B, Panchapakesan R, Full AR, et al. 2009. Generalized serial dilution module for monotonic and arbitrary microfluidic gradient generators. *Lab Chip* 9:709–17

122. Kim C, Lee K, Kim JH, Shin KS, Lee KJ, et al. 2008. A serial dilution microfluidic device using a ladder network generating logarithmic or linear concentrations. *Lab Chip* 8:473–79
123. Jeon NL, Baskaran H, Dertinger SKW, Whitesides GM, Van de Water L, Toner M. 2002. Neutrophil chemotaxis in linear and complex gradients of interleukin-8 formed in a microfabricated device. *Nat. Biotechnol.* 20:826–30
124. Dertinger SKW, Chiu DT, Jeon NL, Whitesides GM. 2001. Generation of gradients having complex shapes using microfluidic networks. *Anal. Chem.* 73:1240–46
125. Amarie D, Glazier JA, Jacobson SC. 2007. Compact microfluidic structures for generating spatial and temporal gradients. *Anal. Chem.* 79:9471–77
126. Lin F, Saadi W, Rhee SW, Wang SJ, Mittal S, Jeon NL. 2004. Generation of dynamic temporal and spatial concentration gradients using microfluidic devices. *Lab Chip* 4:164–67
127. Irimia D, Geba DA, Toner M. 2006. Universal microfluidic gradient generator. *Anal. Chem.* 78:3472–77
128. Shamloo A, Ma N, Poo MM, Sohn LL, Heilshorn SC. 2008. Endothelial cell polarization and chemotaxis in a microfluidic device. *Lab Chip* 8:1292–99
129. Chung BG, Flanagan LA, Rhee SW, Schwartz PH, Lee AP, et al. 2005. Human neural stem cell growth and differentiation in a gradient-generating microfluidic device. *Lab Chip* 5:401–6
130. Saadi W, Wang SJ, Lin F, Jeon NL. 2006. A parallel-gradient microfluidic chamber for quantitative analysis of breast cancer cell chemotaxis. *Biomed. Microdevices* 8:109–18
131. Wang SJ, Saadi W, Lin F, Nguyen CMC, Jeon NL. 2004. Differential effects of EGF gradient profiles on MDA-MB-231 breast cancer cell chemotaxis. *Exp. Cell Res.* 300:180–89
132. Englert DL, Manson MD, Jayaraman A. 2010. Investigation of bacterial chemotaxis in flow-based microfluidic devices. *Nat. Protoc.* 5:864–72
133. Gunawan RC, Silvestre J, Gaskins HR, Kenis PJA, Leckband DE. 2006. Cell migration and polarity on microfabricated gradients of extracellular matrix proteins. *Langmuir* 22:4250–58
134. Keenan TM, Folch A. 2008. Biomolecular gradients in cell culture systems. *Lab Chip* 8:34–57
135. Saadi W, Rhee SW, Lin F, Vahidi B, Chung BG, Jeon NL. 2007. Generation of stable concentration gradients in 2D and 3D environments using a microfluidic ladder chamber. *Biomed. Microdevices* 9:627–35
136. Atencia J, Morrow J, Locascio LE. 2009. The microfluidic palette: a diffusive gradient generator with spatio-temporal control. *Lab Chip* 9:2707–14
137. Sager J, Young M, Stefanovic D. 2006. Characterization of transverse channel concentration profiles obtainable with a class of microfluidic networks. *Langmuir* 22:4452–55
138. Gorman BR, Wikswo JP. 2008. Characterization of transport in microfluidic gradient generators. *Microfluid. Nanofluid.* 4:273–85
139. Wang Y, Mukherjee T, Lin Q. 2006. Systematic modeling of microfluidic concentration gradient generators. *J. Micromech. Microeng.* 16:2128–37
140. Huh D, Matthews BD, Mammoto A, Montoya-Zavala M, Hsin HY, Ingber DE. 2010. Reconstituting organ-level lung functions on a chip. *Science* 328:1662–68
141. Sudo R, Chung S, Zervantonakis IK, Vickerman V, Toshimitsu Y, et al. 2009. Transport-mediated angiogenesis in 3D epithelial coculture. *FASEB J.* 23:2155–64
142. Liu TJ, Li CY, Li HJ, Zeng SJ, Qin JH, Lin BC. 2009. A microfluidic device for characterizing the invasion of cancer cells in 3-D matrix. *Electrophoresis* 30:4285–91
143. Liu TJ, Lin BC, Qin JH. 2010. Carcinoma-associated fibroblasts promoted tumor spheroid invasion on a microfluidic 3D co-culture device. *Lab Chip* 10:1671–77
144. Meyvantsson I, Beebe DJ. 2008. Cell culture models in microfluidic systems. *Annu. Rev. Anal. Chem.* 1:423–49
145. Basmadjian D, Sefton MV, Baldwin SA. 1997. Coagulation on biomaterials in flowing blood: some theoretical considerations. *Biomaterials* 18:1511–22
146. Shen F, Kastrup CJ, Ismagilov RF. 2008. Using microfluidics to understand the effect of spatial distribution of tissue factor on blood coagulation. *Thromb. Res.* 122:S27–30
147. Shen F, Pompano RR, Kastrup CJ, Ismagilov RF. 2009. Confinement regulates complex biochemical networks: initiation of blood clotting by "diffusion acting". *Biophys. J.* 97:2137–45

148. Kastrup CJ, Runyon MK, Lucchetta EM, Price JM, Ismagilov RF. 2008. Using chemistry and microfluidics to understand the spatial dynamics of complex biological networks. *Acc. Chem. Res.* 41:549–58

149. Kastrup CJ, Runyon MK, Shen F, Ismagilov RF. 2006. Modular chemical mechanism predicts spatiotemporal dynamics of initiation in the complex network of hemostasis. *Proc. Natl. Acad. Sci. USA* 103:15747–52

Annual Review of
Analytical Chemistry

Volume 4, 2011

Contents

Indexes

Errata

An online log of corrections to the *Annual Review of Analytical Chemistry* articles may be found at http://arjournals.annualreviews.org/errata/anchem